Fourier transforms, (B1) and (B13) differ for $\mu=0$ only by $\tilde{\Gamma}_0$ being replaced by $\Gamma D_0^{-1}D$. Hence, the relation

$$\tilde{\Gamma}_0(p,q)=D_0^{-1}(q)D(q)\Gamma(p,q) \qquad (B14)$$

is valid.

If we assume that $\tilde{\Gamma}_\mu(p,q)$ is analytic in q so that $\mathbf{q}\cdot\tilde{\Gamma}(p,q)$ vanishes for $\mathbf{q}\to 0$, we need only show $D^{-1}(q)D_0(q)=1$ in the limit $\mathbf{q}\to 0$, in order to prove (4.3). The relation $q_0\Gamma(p,q)=G^{-1}(p+q)-G^{-1}(p)$ then follows from (B5), (B14) in the limit $\mathbf{q}\to 0$. To prove

$D^{-1}(q_0)D_0(q_0)=1$ or equivalently $D_0^{-1}(q_0)D(q_0)=1$ we use Eq. (B12):

$$D_0^{-1}(\mathbf{q},t)D(\mathbf{q};t,t')=\delta(t-t')-ig(\mathbf{q})\langle T\rho(\mathbf{q},t)\,\varphi^\dagger(\mathbf{q},t')\rangle,$$

where $D(\mathbf{q};t,t')\equiv-i\langle T\{\varphi(\mathbf{q},t)\varphi^\dagger(\mathbf{q},t')\}\rangle$. Now for $\mathbf{q}=0$, $\rho(\mathbf{q},t)=N(t)=N$ is a constant of the motion, i.e., the total number of electrons. Thus,

$$q_0[D_0^{-1}(q_0)D(q_0)-1]=0$$

which completes our proof.

Dynamical Motion and Gamma-Ray Cross Section of an Impurity Nucleus in a Crystal. I. Isolated Impurities in Germanium and Aluminum

G. W. Lehman and R. E. DeWames

North American Aviation Science Center, Canoga Park, California

(Received 20 March 1963)

The general theory of the dynamical motion and gamma-ray cross section for a single impurity nucleus harmonically coupled to an arbitrary collection of N atoms is developed in supermatrix representation. The relevant properties of the system are expressed in terms of a functional matrix $f_0(\boldsymbol{\Omega})$ of order $3N\times 3N$, where $\boldsymbol{\Omega}$ is the mass-reduced force-constant matrix. Our approach is to use a Cauchy singular integral representation for $f_0(\boldsymbol{\Omega})$ involving an integration along the real frequency, ω, axis. Matrix partitioning techniques are used to reduce our problem to one of evaluating the 3×3 impurity atom dynamic response matrix, $\{G\}_{11}=(1+\epsilon)[I_3+\tau\epsilon A_{11}]^{-1}A_{11}$, where $\tau=\omega^2-i\delta$. Here, δ is an arbitrarily small number, and $\epsilon+1=$ ratio of impurity atom to host atom mass, (M_I/M_H). For an arbitrary physical arrangement of the atoms, $A_{11}=\{[I_{3(z+1)}-D_{z+1}(\Delta F/M_H)]^{-1}D_{z+1}\}_{11}$, where the subscript, 1, refers to the impurity atom coordinates, ΔF is the perturbation in force-constant matrix, and z is the number of sites over which the perturbation extends. The D_{z+1} matrix has matrix elements obtained from the elements of the pure host matrix $D_H=[\tau I_{3N}-F_HM_H^{-1}]^{-1}$, F_H is the pure host force-constant matrix. I_k is a $k\times k$ unit matrix.

The general approach is used to study the dynamic response of an impurity atom substituted in the aluminum lattice with arbitrary ϵ and nearest neighbor ΔF. The A matrix is block diagonalized by introducing the molecular vibration symmetry coordinates and A_{11} is characterized by a 4×4 symmetry adapted Green's function matrix whose elements have been tabulated. A generalized tensor force-constant model is used with Walker's force constants characterizing D_H, the pure aluminum lattice Green's function matrix. Similar studies are carried out for a Sn^{119} atom isotopically substituted in Ge, where the relevant Green's functions are derived from Phillip's frequency spectrum.

The dynamical motion and gamma-ray cross section of impurity nuclei are characterized by a dynamic response function, K, which is related to the imaginary part of $\{G\}_{11}$. Typical K functions are presented for Fe^{57} in Al for various changes in ΔF and for Sn^{119} in Ge with $\Delta F=0$. Our results show that the dynamical behavior of impurity atoms in real lattices is quite sensitive to the vibrational properties of the host lattice. The resonant fraction of γ rays absorbed by the impurity nucleus, f, the Lamb-Mössbauer coefficient, $2W$, and mean-square velocity, $(v_I^2)_{av}$, of Fe^{57}-Al are tabulated for several ΔF changes as a function of temperature. Our results are extrapolated to study the temperature dependence of $2W$ and f for Fe^{57}-Cu and Fe^{57}-Pt. From the results derived in this paper, it is possible to determine K, $2W$, and $(v_I^2)_{av}$ for any ϵ and ΔF for Al as a host lattice.

I. INTRODUCTION

THE purpose of this paper is to present the results of detailed studies of the dynamical motion and γ-ray cross section of a Mössbauer impurity nucleus bound in a locally perturbed host crystal at an arbitrary temperature.[1] A completely general lattice dynamics model is assumed in which the impurity nucleus is harmonically coupled to the host lattice with force constants which differ from those of the pure host lattice.

A considerable amount of research has been carried out on vibrational as well as electronic impurity states in crystals. Green's function approaches to these problems appear to have been developed by Lifshitz,[2] Koster

[1] For a recent review article on the Mössbauer effect see H. Frauenfelder, *The Mössbauer Effect* (W. A. Benjamin, Inc., New York, 1962). Studies of a general nature involving impurity atom motion, resonant Mössbauer absorption by impurity nuclei, and optical absorption by impurity vibrational modes have been carried out by A. A. Maradudin, in Lecture Notes of Brandeis University 1962 Summer Institute of Theoretical Physics [W. A. Benjamin, Inc. (to be published)].

[2] Qualitative studies of the impurity vibrational problem have been carried out by I. M. Lifshitz and co-workers in Russia over the past twenty years. See I. M. Lifshitz, Suppl. Nuovo Cimento 3, 733 (1956) for references to prior work.

and Slater,[3] and Lax,[4] independently. Techniques have also been developed by Lifshitz,[2] Montroll and Potts,[5] and Mahanty, Maradudin, and Weiss[6] which enable one to compute changes in thermodynamic functions in terms of contour integrals involving the host-lattice Green's functions. This approach has been used by Wallis and Maradudin[7] to calculate the optical absorption associated with an impurity vibrational mode in a linear chain. Maradudin, Flinn, and Ruby[8] have used these techniques to compute the mean-square velocity of an atom substituted into the lattice isotopically. They[9] have also calculated the mean-square displacement of an impurity atom valid at temperatures in the vicinity of the Debye temperature and above.

Brout and Visscher[10] have pointed out that one might observe a Mössbauer pip associated with a virtual bound mode in the continuum arising from the isotopic substitution of a heavy-mass Mössbauer nuclei into a light-mass host lattice. Lehman and DeWames,[11] using techniques described in this paper, have calculated the cross section for the virtual mode considered by Brout and Visscher and find it to be quite small.

Visscher[12] has recently studied the resonant absorption of gamma rays by impurity nuclei using a nearest neighbor central-force model for a simple cubic lattice. The motivation for this approach apparently lies in the fact that the mathematical development is fairly simple. However, our goal is to use the Mössbauer effect to gain insight into the coupling of a substitutional impurity atom with its surrounding host-lattice atoms. Consequently, our studies have been focused on those host lattices whose phonon spectra have been determined by neutron or x-ray diffraction methods.

In Sec. II of this paper, we show that the problem of determining the dynamical motion and γ-ray cross section of a single impurity nucleus harmonically bound to $N-1$ other atoms can be formulated in supermatrix representation. This formulation leads to the necessity of evaluating a 3×3 submatrix (associated with the impurity-atom motion) which is obtained from a $3N\times3N$ matrix function $f_0(\mathbf{\Omega})$, where $\mathbf{\Omega}^2=\mathbf{M}^{-1/2}\mathbf{F}\mathbf{M}^{-1/2}$, $\mathbf{M}$ and $\mathbf{F}$ are the mass matrix and force constant matrices, respectively. The customary practice[2,6] of representing $f_0(\mathbf{\Omega})$ as a contour integral enclosing the eigenvalues of $\mathbf{\Omega}$ and excluding the poles

of $f_0(\omega)$, where ω is a complex frequency variable, breaks down for our dynamical motion and cross-section problem since the $f_0(\omega)$'s involved are unbounded off the real axis. Consequently, our approach is to use a Cauchy singular integral representation involving an integration over the real frequency axis. Procedures of this type have also been used by other workers, notably in field theoretic problems. The details of our approach appear new and are designed for the problem at hand. Briefly, our problem reduces to that of obtaining a simple representation of $\{\mathbf{G}(\tau)\}_{11}=\{[\tau\mathbf{I}_{3N}-\mathbf{\Omega}^2]^{-1}\}_{11}$, where $\tau=\omega^2-i\delta$, $\mathbf{I}_{3N}$ is a $3N\times3N$ identity matrix, the subscript on the curly bracket refers to the 3×3 impurity atom submatrix obtained from the $3N\times3N$ supermatrix $\mathbf{G}$, and δ is a small positive number which is set equal to zero after the integration is carried out. We use partitioning techniques, whose importance has recently been stressed by Löwdin (see Ref. 21), to establish the remarkably simple result that $\{\mathbf{G}(\tau)\}_{11}=(1+\epsilon)[\mathbf{I}_3+\tau\epsilon\mathbf{A}_{11}]^{-1}\mathbf{A}_{11}$, where $\epsilon+1=M_I/M_H$, where M_H and M_I denote host and impurity atom masses, respectively, and $\mathbf{A}$ is $\mathbf{G}$ when the impurity atom mass is M_H. The $\mathbf{A}$ matrix, in turn, can be expressed in terms of the host $\mathbf{G}_H$ and a matrix $\Delta\mathbf{F}$ describing the perturbation in $\mathbf{F}$ introduced by the presence of the impurity atom. Further simplification results when the host assembly forms a periodic lattice. In this case, one should introduce molecular vibration symmetry coordinates as basis functions and construct the matrix elements of $\mathbf{G}_H$ in this basis. The total number of symmetry coordinates is $3(z+1)$, where z is the number of perturbed neighboring atoms of the impurity atom. The 3×3 $\mathbf{A}_{11}$ matrix is then expressed in terms of a symmetry adapted Green's function matrix whose order is equal to number of symmetry coordinates which couple to the impurity atom motion. This motion is characterized by a dynamical response function, K, which depends upon frequency. This function has the valuable property of always being normalized to unity. We also establish in this section that the gamma-ray cross section, mean square displacement, and mean-square velocity of the impurity nucleus are simply related to averages over the K function.

In Sec. III, the general formulas of Sec. II are used to calculate the dynamic response function, K, for a Sn^{119} atom isotopically substituted into the germanium lattice. The Green's function for this problem is tabulated using Phillip's frequency spectrum[13] for germanium obtained from Brockhouse and Iyengar's neutron data.[14] The temperature dependence of the Lamb-Mössbauer coefficient,[1] $2W$, is calculated for the $Ge-Sn^{119}$ problem and compared with experimental and theoretical calculations of $Sn-Sn^{119}$.

In Sec. IV, we consider the general problem of determining the K function for an impurity nucleus substituted in the aluminum lattice. A complete character-

[3] G. F. Koster and J. C. Slater, Phys. Rev. 94, 1392 (1954); 95, 1167 (1954).
[4] M. Lax, Phys. Rev. 94, 1391 (1954).
[5] E. W. Montroll and R. B. Potts, Phys. Rev. 100, 525 (1955); 102, 72 (1956).
[6] J. Mahanty, A. A. Maradudin, and G. Weiss, Progr. Theoret. Phys. (Kyoto) 20, 369 (1958).
[7] R. F. Wallis and A. A. Maradudin, Progr. Theoret. Phys. (Kyoto) 24, 1055 (1960).
[8] A. A. Maradudin, P. Flinn, and S. Ruby, Phys. Rev. 126, 9 (1962).
[9] A. A. Maradudin and P. Flinn, Phys. Rev. 126, 2059 (1962).
[10] R. Brout and W. Visscher, Phys. Rev. Letters 9, 54 (1962).
[11] G. W. Lehman and R. E. DeWames, Phys. Rev. Letters 9, 344 (1962).
[12] W. M. Visscher, Phys. Rev. 129, 28 (1963).

[13] J. C. Phillips, Phys. Rev. 113, 147 (1959).
[14] B. N. Brockhouse and P. K. Iyengar, Phys. Rev. 111, 747 (1958).

izization of the vibrational spectrum associated with this general impurity problem requires 39 symmetry coordinates. Fortunately, the Green's function for this problem transforms according to the full cubic group and only three impurity modes associated with arbitrary changes in nearest-neighbor force constants couple to the impurity nucleus. Consequently, a 4×4 Green's function symmetry adapted matrix is needed in order to calculate the dynamical behavior of the impurity nucleus. This Green's function matrix is tabulated using Walker's generalized tensor force model for aluminum derived from x-ray data.[15] Detailed calculations of the dynamic response function for Al–Fe⁵⁷ are also presented in graphical form. The temperature dependence of the Lamb-Mössbauer coefficient, $2W$, is also given for various changes in first-neighbor force constants of the Fe⁵⁷ nucleus. By appropriate scaling of the frequency spectrum, we also study the cases Cu—Fe⁵⁷ and Pt—Fe⁵⁷.

II. GENERAL THEORETICAL CONSIDERATIONS

As a prelude to deriving formulas which enable us to calculate the Mössbauer absorption coefficient of an impurity nucleus bound harmonically to N atoms in a crystal, we consider the classical motion of an impurity nucleus of mass, M_I, which has received a momentum transfer $\mathbf{p}_1$ at time, $t=0$. We denote the amplitude of motion of the N atoms in terms of a supervector, $\mathbf{y}=(\mathbf{y}_1,\mathbf{y}_2,\cdots,\mathbf{y}_N)$, where $\mathbf{y}_i$ refers to the harmonic displacement of the ith atom. The subscript $i=1$ always refers to the impurity atom; similarly, the next z subscripts label the z nearest neighbor atoms. The equations of motion of our N coupled atoms are

$$\mathbf{M}\ddot{\mathbf{y}}(t) = -\mathbf{F}\mathbf{y}(t),\qquad(1)$$

where $\mathbf{M}$ and $\mathbf{F}$ are the mass and force-constant supermatrices.[16] The mass supermatrix is diagonal with a block of 3×3 matrices on the diagonal denoted by

$$\mathbf{M}_{ij}=\delta_{ij}M_I\mathbf{I}_3,\quad i,j=1,2,3\qquad(2)$$

$$\mathbf{M}_{ij}=\delta_{ij}M_H\mathbf{I}_3,\quad i,j>3,\qquad(3)$$

where M_H refers to the mass of a host-lattice atom, and $\mathbf{I}_3$ is a 3×3 identity matrix. Dots over $\mathbf{y}(t)$ in Eq. (1) and elsewhere refer to time differentiation. The time dependence of the momentum of the N atoms will be denoted by

$$\mathbf{p}(t)\equiv\mathbf{M}\dot{\mathbf{y}}(t).\qquad(4)$$

Equation (1) is to be solved under the boundary conditions

$$\mathbf{p}(0)=(\mathbf{p}_1,0,0,\cdots,0),$$
$$\mathbf{y}(0)=(0,0,\cdots,0),\qquad(5)$$

where $\mathbf{0}$ is a 3-component null vector.

[15] C. B. Walker, Phys. Rev. 103, 547 (1956).
[16] We follow the convention that all nonsubscripted bold-face symbols are supervectors or supermatrices; similarly, double-subscripted bold-faced symbols are 3×3 matrices and single-subscripted bold-faced symbols are 3-component vectors, with the exception that o is always a 3-component null vector.

A. Time Dependence of Impurity Atom Momentum

We now recall that the eigenvalues of $\mathbf{F}$ are positive definite. Hence, we can construct the positive square-root symmetric matrix

$$\mathbf{\Omega}=(\mathbf{M}^{-1/2}\mathbf{F}\mathbf{M}^{-1/2})^{1/2},\qquad(6)$$

and obtain a formal solution to Eq. (1) which vanishes at $t=0$ given by

$$\mathbf{y}(t)=\mathbf{M}^{-1/2}\mathbf{\Omega}^{-1}\sin(\mathbf{\Omega}t)\mathbf{M}^{-1/2}\mathbf{p}(0).\qquad(7)$$

The matrix operator $\mathbf{\Omega}^{-1}\sin(\mathbf{\Omega}t)$ has a unique representation in power-series form since the eigenvalue spectrum of $\mathbf{\Omega}$ is bounded. One can also express this operator in spectral form using the eigenfunctions of $\mathbf{\Omega}$. However, the formal development is more compact in matrix form. The solution given by Eq. (7) satisfies the second boundary condition $\mathbf{M}\dot{\mathbf{y}}(0)=\mathbf{p}(0)$. Our final result for $\mathbf{p}$, obtained from Eqs. (4) and (7), is

$$\mathbf{p}(t)=\mathbf{M}^{1/2}\cos(\mathbf{\Omega}t)\mathbf{M}^{-1/2}\mathbf{p}(0),\qquad(8)$$

so that the momentum of the impurity atom is given by

$$\mathbf{p}_1(t)=\{\cos(\mathbf{\Omega}t)\}_{11}\mathbf{p}_1(0),\qquad(9)$$

where $\{\ \}_{11}$ refers to the 3×3 matrix associated with the impurity atom in the supermatrix representation of $\cos(\mathbf{\Omega}t)$.

An explicit representation of $\cos(\mathbf{\Omega}t)$ suitable for the impurity atom problem will be developed in Sec. II C.

B. Formulas for Calculating Mössbauer Cross Sections for an Impurity Nucleus

Lamb[17] has derived the absorption and emission cross section for a process in which momentum is suddenly transferred to an atom of the lattice and Mössbauer[18] has applied this theory to the resonant absorption of gamma rays in crystals. Kaufman and Lipkin[19] have re-examined Lamb's treatment and show that his approximate formulas are, in fact, exact. The derivation given by Kaufman and Lipkin is valid for an arbitrary collection of N atoms harmonically bound. The total cross section for absorption of a gamma ray having momentum, $\mathbf{p}_1$, by an impurity nucleus of mass, M_I, can be written as

$$W(E)=\left(\frac{2}{\Gamma}\right)\mathrm{Re}\int_0^\infty d\mu$$
$$\times\exp[-\mu(\tfrac{1}{2}\Gamma)+i\mu(E-E_0)]e^{g(\mu)},\qquad(10)$$

where E_0 is the energy difference between excited and ground state of the nucleus, Γ is the natural linewidth

[17] W. E. Lamb, Phys. Rev. 55, 190 (1939).
[18] R. L. Mössbauer, Z. Physik 151, 124 (1958). Also see Ref. 1.
[19] B. Kaufman and H. J. Lipkin, Ann. Phys. (N.Y.) 18, 294 (1962).

of the nuclear excited state, and E is the energy of the gamma ray. The function $g(\mu)$ is given by

$$2g(\mu) = -\sum_{s=1}^{3N} \sigma_s^2 \left\{ \frac{1+\gamma_s}{1-\gamma_s} - \frac{x_s^{-1}+\gamma_s x_s}{1-\gamma_s} \right\}, \quad (11)$$

where

$$\gamma_s = \exp(-\hbar\omega_s/kT) \quad \text{and} \quad x_s = \exp(+i\hbar\omega_s\mu), \quad (12)$$

and

$$\sigma_s^2 = (\mathbf{p}_1 \cdot \mathbf{u}_{1s})^2 / (\hbar\omega_s M_I). \quad (13)$$

The vector $\mathbf{u}_{1s}$ denotes the amplitude of the impurity atom in the sth mode belonging to the frequency ω_s. The ω_s's are eigenvalues of the $\mathbf{\Omega}$ matrix defined by Eq. (6). Since $\mathbf{u}_{1s}$ is the element of the supervector of the generalized amplitude function, $\mathbf{y}_s$, associated with the impurity atom motion, where

$$\mathbf{\Omega}\mathbf{y}_s = \omega_s \mathbf{y}_s, \quad (14)$$

we can write

$$2g(\mu) = \sum_{s=1}^{3N} (\mathbf{p}_1 \cdot \mathbf{u}_{1s})^2 H(\omega_s)$$

$$= \sum_{s=1}^{3N} [\mathbf{p}_1 \cdot H(\omega_s)\mathbf{u}_{1s}][\mathbf{u}_{1s} \cdot \mathbf{p}_1], \quad (15)$$

for suitably defined $H(\omega_s)$, see Eq. (11) or Eq. (17) below. Setting $\mathbf{p} = (\mathbf{p}_1, 0, \cdots, 0)$, it follows that $\mathbf{p}_1$ and $\mathbf{u}_{1s}$ can be replaced by $\mathbf{p}$ and $\mathbf{y}_s$, respectively. Now, formally $H(\omega_s)\mathbf{y}_s \equiv H(\mathbf{\Omega})\mathbf{y}_s$, and since the $\mathbf{y}_s$, $s = 1, 2, \cdots, 3N$, form a complete set of orthonormal vectors, one has

$$\sum_s (\mathbf{a} \cdot \mathbf{A}\mathbf{y}_s)(\mathbf{y}_s \cdot \mathbf{a}) = (\mathbf{a} \cdot \mathbf{A}\mathbf{a}).$$

Consequently, Eq. (15) can be written as

$$2g(\mu) = [\mathbf{p} \cdot H(\mathbf{\Omega})\mathbf{p}] \equiv [\mathbf{p}_1 \cdot \{H(\mathbf{\Omega})\}_{11}\mathbf{p}_1]. \quad (16)$$

From Eqs. (11) and (13), one can write

$$H(\omega) = (1/zM_I)[(\cos\mu z - 1)\coth(z/2kT) - i\sin\mu z], \quad (17)$$

where $z = \hbar\omega$.

Consequently, $g(\mu)$ can be determined from the 3×3 matrix $\{H(\mathbf{\Omega})\}_{11}$. One should also note that $H(\omega)$ is bounded along the real frequency axis, is an analytic function for all $0 < T < \infty$, and has simple poles at $z_m = 2\pi i m kT$ on the imaginary axis, where m^2 is an integer.

C. Integral Representation of Matrix Operators Associated with Impurity-Atom Motion

In order to calculate $\mathbf{p}_1(t)$ and $g(\mu)$, we need an explicit representation for the 3×3 matrices, $\{\cos(\mathbf{\Omega}t)\}_{11}$ and $\{H(\mathbf{\Omega})\}_{11}$, which are even functions of their argument, $\mathbf{\Omega}$. We now develop an integral representation of a matrix operator $f_0(\mathbf{\Omega})$ in terms of $f_0(|\tau|^{1/2})$ for

$-\infty < \tau < \infty$. This approach avoids the usual pitfalls of contour integral techniques for functions which are unbounded when one goes off the real axis as is the case here when μ or $t \to \infty$. We note that for $f_0(x)$ continuous, $f_0(-x) = f_0(x)$, and bounded for $-\infty < x < \infty$, one has

$$\frac{1}{2\pi i} \lim_{\delta \to 0} \int_{-\infty}^{\infty} d\tau f_0(|\tau|^{1/2})\{[\tau - i\delta - x^2]^{-1} - [\tau + i\delta - x^2]^{-1}\}$$

$$= \frac{1}{\pi} \lim_{\delta \to 0} \int_{-\infty}^{\infty} d\tau f_0(|\tau|^{1/2}) \frac{\delta}{(\tau - x^2)^2 + \delta^2},$$

$$= f_0(x), \quad (18)$$

according to Cauchy's well-known singular integral theorem.[20] Since all of the functions discussed in this paper are bounded and continuous on the real axis, we can replace x by $\mathbf{\Omega}$ in the first line of Eq. (18) and obtain a useful representation of a large class of matrix operators. Hence, we have established, using Eqs. (6) and (18), that

$$f_0(\mathbf{\Omega}) = (1/\pi) \lim_{\delta \to 0} \int_{-\infty}^{\infty} d\tau f_0(|\tau|^{1/2}) \operatorname{Im}\mathbf{G}(\tau - i\delta), \quad (19)$$

where

$$\mathbf{G}(\tau) = [\tau \mathbf{I}_{3N} - \mathbf{M}^{-1/2}\mathbf{F}\mathbf{M}^{-1/2}]^{-1} \quad (20)$$

and Im stands for the imaginary part of the expression which follows it.

In order to obtain $\mathbf{p}_1(t)$ and $g(\mu)$, we simply need

$$\{\mathbf{G}(\tau)\}_{11} = \{[\tau \mathbf{I}_{3N} - \mathbf{M}^{-1/2}\mathbf{F}\mathbf{M}^{-1/2}]^{-1}\}_{11}, \quad (21)$$

that is, the 3×3 matrix associated with the impurity atom.

We now set

$$\mathbf{M} = M_H \mathbf{I}_{3N} + \Delta\mathbf{M} \quad (22)$$

and

$$\mathbf{F} = \mathbf{F}_H + \Delta\mathbf{F}, \quad (23)$$

$$\mathbf{D}_H(\tau) = [\tau \mathbf{I}_{3N} - \mathbf{F}_H M_H^{-1}]^{-1}, \quad (24)$$

where the subscript, H, refers to the pure host lattice. By straightforward matrix manipulation, one finds, using Eqs. (21), (22), (23), and (24), that

$$[\tau \mathbf{I}_{3N} - \mathbf{M}^{-1/2}\mathbf{F}\mathbf{M}^{-1/2}]^{-1}$$
$$= \mathbf{M}^{1/2}[\mathbf{I}_{3N} + \mathbf{A}\tau(\Delta\mathbf{M}/M_H)]^{-1}\mathbf{A}\mathbf{M}^{1/2}M_H^{-1}, \quad (25)$$

where

$$\mathbf{A} = [\mathbf{I}_{3N} - \mathbf{D}_H(\Delta\mathbf{F}/M_H)]^{-1}\mathbf{D}_H. \quad (26)$$

In deriving Eq. (25), we have used the fact that

$$[\mathbf{B}^{-1}\mathbf{C} + \mathbf{I}_{3N}]^{-1} \equiv [\mathbf{B} + \mathbf{C}]^{-1}\mathbf{B}$$

for arbitrary $\mathbf{C}$ and nonsingular $\mathbf{B}$. Next, we obtain a simple form for the inverse matrix shown on the right

[20] E. C. Titchmarsh, *Introduction to the Theory of Fourier Integrals* (Oxford University Press, London 1937), p. 30.

side of Eq. (25) by using partitioning techniques.[21] In supermatrix form, one has

$$\mathbf{A} = \begin{pmatrix} \mathbf{A}_{11}, & \mathbf{A}_{1b} \\ \mathbf{A}_{b1}, & \mathbf{A}_{bb} \end{pmatrix}, \qquad (27)$$

where the subscript 1 refers to the impurity atom and b refers to the remaining $N-1$ atoms of the crystal. By direct construction, one finds that

$$\left[\mathbf{I}_{3N} + \mathbf{A}\tau \frac{\Delta \mathbf{M}}{M_H} \right]^{-1} = \begin{pmatrix} \mathbf{I}_3 + \mathbf{A}_{11}\tau\epsilon, & \mathbf{0} \\ \mathbf{A}_{b1}\tau\epsilon, & \mathbf{I}_b \end{pmatrix}^{-1}, \qquad (28)$$

where

$$\epsilon = (M_I/M_{II}) - 1, \qquad (29)$$

and $\mathbf{0}$ is a $3 \times 3(N-1)$ null matrix. By inspection, one notes that

$$\mathbf{B} = \begin{pmatrix} \mathbf{B}_{11}, & \mathbf{0} \\ \mathbf{B}_{b1}, & \mathbf{I}_b \end{pmatrix}^{-1} = \begin{pmatrix} \mathbf{B}_{11}^{-1}, & \mathbf{0} \\ -\mathbf{B}_{b1}\mathbf{B}_{11}^{-1}, & \mathbf{I}_b \end{pmatrix}, \qquad (30)$$

since $\mathbf{B}\mathbf{B}^{-1} = \mathbf{B}^{-1}\mathbf{B} \equiv \mathbf{I}_{3N}$. Hence, when the previous results are combined one obtains from Eq. (21)

$$\{\mathbf{G}(\tau)\}_{11} = (1+\epsilon)\mathbf{A}_{11}[\mathbf{I}_3 + \mathbf{A}_{11}\tau\epsilon]^{-1}, \qquad (31)$$

where

$$\mathbf{A}_{11} = \{[\mathbf{I}_{3N} - \mathbf{D}_H(\Delta \mathbf{F}/M_H)]^{-1}\mathbf{D}_H\}_{11}, \qquad (32)$$

is the 3×3 matrix associated with the impurity atom in the supermatrix representation of $\mathbf{A}$.

Equations (31) and (32) are completely general and hold for arbitrary $\Delta \mathbf{F}$, $(\mathbf{F}_H/M_H)$ and ϵ for an arbitrary collection of N harmonically coupled atoms. An inspection of our integral theorem, Eq. (19), now shows that

$$\lim_{\delta \to 0} \mathrm{Im} \frac{1}{\pi} \int_{-\infty}^{\infty} d\tau \{\mathbf{G}(\tau - i\delta)\}_{11} \equiv \mathbf{I}_3, \qquad (33)$$

a result obtained by setting $f_0(|\tau|^{1/2}) = 1$.

1. Force-Constant Perturbation Restricted to z Sites

In practice, one restricts the perturbation in $\mathbf{F}$ to atoms in the neighborhood of the impurity atom. If z denotes the number of atoms over which the perturbation extends relative to the impurity atom, then $\mathbf{A}_{11}$ is considerably simplified. Using steps analogous to the construction of Eq. (28), one readily finds that

$$\mathbf{A}_{11} = \{[\mathbf{I}_{3(z+1)} - \mathbf{D}_{z+1}(\Delta \mathbf{F}/M_H)]^{-1}\mathbf{D}_{z+1}\}_{11}, \qquad (34)$$

where $\mathbf{D}_{z+1}$ is a $3(z+1) \times 3(z+1)$ matrix obtained from the appropriate $3(z+1)$ elements of $\mathbf{D}_H$[Eq. (24)].

[21] Per-Olov Löwdin, *Studies in Perturbation Theory. IV. Solution of Eigenvalue Problem by Projection Operator Formalism* (Quantum Chemistry Group, Uppsala University, Uppsala, Sweden, 1960).

2. Construction of $\mathbf{D}_{z+1}$ for a Cubic Crystal

We now pass on to the case of an arbitrary cubic crystal lattice and take our impurity atom to be located at the center. The most convenient description of the motion of the atoms is given by using a supermatrix representation for $\mathbf{D}_{z+1}$. We denote the (j,k) element of $\mathbf{D}_{z+1}$ by a 3×3 matrix, $\mathbf{d}_{jk}$, where j and k refer to the positions of the impurity and z perturbed sites. Using periodic boundary conditions it is easy to show that[9]

$$\mathbf{d}_{jk} = N^{-1} \sum_{\mathbf{q}} [\tau \mathbf{I}_3 - \mathbf{\Lambda}(\mathbf{q})]^{-1} \exp[i\mathbf{q} \cdot (\mathbf{R}_j - \mathbf{R}_k)], \qquad (35)$$

where $\mathbf{q}$ labels the N (continuum) propagation vectors which range over the appropriate reduced Brillouin zone, $\mathbf{R}_j$ denotes the position of the jth atom, and

$$\mathbf{\Lambda}(\mathbf{q}) = \sum_{\mathbf{R}_j \neq 0} [1 - \exp(-i\mathbf{q} \cdot \mathbf{R}_j)]\mathbf{F}(\mathbf{R}_j)M_H^{-1}. \qquad (36)$$

The form of Eq. (36) arises from the fact that the (j,k) element of the force-constant supermatrix, $\mathbf{F}_H$, depends only upon $\mathbf{R}_j - \mathbf{R}_k$, i.e.,

$$\{\mathbf{F}_H\}_{jk} = \mathbf{F}(\mathbf{R}_j - \mathbf{R}_k). \qquad (37)$$

The polarization vectors, $\boldsymbol{\xi}_k$, and frequencies, $\omega_{\mathbf{q}k}$, are obtained by solving

$$\mathbf{\Lambda}(\mathbf{q})\boldsymbol{\xi}_k = (\omega_{\mathbf{q}k})^2 \boldsymbol{\xi}_k. \qquad (38)$$

Physically, it is obvious that $\mathbf{D}_{z+1}$ transforms according to the group of operations associated with the positions of the z atoms relative to the impurity atom. Equation (35) involves a summation over the entire reduced Brillouin zone. It can be shown that $[\tau \mathbf{I}_3 - \mathbf{\Lambda}]^{-1}$ transforms like $\mathbf{\Lambda}(\mathbf{q})$ with respect to rotational operators on $\mathbf{q}$. The symmetry properties of $\mathbf{\Lambda}(\mathbf{q})$ are identical to those of

$$\mathbf{\Lambda}_0(\mathbf{q}) \propto \begin{bmatrix} q_x^2, & q_x q_y, & q_x q_z \\ q_x q_y, & q_y^2, & q_y q_z \\ q_x q_z, & q_y q_z, & q_z^2 \end{bmatrix}, \qquad (39)$$

which is a special case of $\mathbf{\Lambda}$ in the long-wavelength limit. Hence, the symmetry properties associated with $\mathbf{d}_{jk}$ [Eq. (35)] are identical to

$$\mathbf{d}_0(\mathbf{R}) = \sum_{\mathbf{q}} \mathbf{\Lambda}_0 \exp[i\mathbf{q} \cdot \mathbf{R}], \qquad (40)$$

which can be written as

$$-\mathbf{d}_0(\mathbf{R}) = \begin{bmatrix} \partial_{xx}, & \partial_{xy}, & \partial_{xz} \\ \partial_{xy}, & \partial_{yy}, & \partial_{yz} \\ \partial_{xz}, & \partial_{yz}, & \partial_{zz} \end{bmatrix} \sum_{\mathbf{q}} \exp(i\mathbf{q} \cdot \mathbf{R}), \qquad (41)$$

where $\partial_{xx} = \partial^2/\partial x^2$, $\partial_{xy} = \partial^2/\partial x \partial y$, etc. The sum in Eq. (41) belongs to the completely symmetrical or Γ_1 representation with respect to symmetry operations on $\mathbf{R}$ (as can be seen by making a power-series expansion of the exponential factor) and we conclude that $\mathbf{d}_{jk}$ has

transformation properties isomorphic to the transformation properties of

$$\begin{bmatrix} x_{jk}^2, & x_{jk}y_{jk}, & x_{jk}z_{jk} \\ x_{jk}y_{jk}, & y_{jk}^2, & y_{jk}z_{jk} \\ x_{jk}z_{jk}, & y_{jk}z_{jk}, & z_{jk}^2 \end{bmatrix}, \qquad (42)$$

where the x_{jk}, y_{jk}, z_{jk} denote the differences between the Cartesian components of $\mathbf{R}_j$ and $\mathbf{R}_k$. Equation (42) is simply a bond-stretching molecular vibration force-constant matrix. This proves our previous assertion concerning the transformation properties of $\mathbf{D}_{z+1}$.

3. Construction of $\mathbf{D}_1$ for Diamond Lattice

We now construct $\mathbf{D}_1$ for a lattice having the diamond structure. One easily finds that

$$\mathbf{D}_1 = N^{-1} \sum_q \{[\tau \mathbf{I}_6 - \mathbf{\Lambda}(\mathbf{q})]^{-1}\}_{11}, \qquad (43)$$

where

$$\mathbf{\Lambda} = \begin{pmatrix} \mathbf{\Lambda}_{11} & \mathbf{\Lambda}_{12} \\ \mathbf{\Lambda}_{12}^* & \mathbf{\Lambda}_{11} \end{pmatrix}. \qquad (44)$$

The asterisk on $\mathbf{\Lambda}_{12}$ denotes a complex conjugate transpose operation. The Bravais lattice for a diamond structure is face-centered cubic. The 3×3 matrix $\mathbf{\Lambda}_{11}$ refers to atom motion on the same lattice, while $\mathbf{\Lambda}_{12}$ refers to coupling of the two sublattices. Clearly,

$$[\tau \mathbf{I}_6 - \mathbf{\Lambda}]^{-1} = \begin{pmatrix} \mathbf{B}_{11} & \mathbf{B}_{12} \\ \mathbf{B}_{21} & \mathbf{B}_{11} \end{pmatrix}, \qquad (45)$$

and one can show by partitioning that

$$\mathbf{B}_{11} = \{\tau \mathbf{I}_3 - \mathbf{\Lambda}_{11} - \mathbf{\Lambda}_{12}^*[\tau \mathbf{I}_3 - \mathbf{\Lambda}_{11}]^{-1}\mathbf{\Lambda}_{12}\}^{-1}. \qquad (46)$$

The symmetry properties of this matrix in $\mathbf{q}$ space are isomorphic to the symmetry properties of $\mathbf{\Lambda}_0$, defined by Eq. (39). The simplest way to visualize this is examine the long-wavelength limit, where $\mathbf{\Lambda}_{11}$ is proportional to $\mathbf{I}_3$ and

$$\mathbf{\Lambda}_{12} = \begin{bmatrix} c_1 & ic_2q_z & ic_2q_y \\ ic_2q_z & c_1 & ic_2q_x \\ ic_2q_y & ic_2q_x & c_1 \end{bmatrix}, \qquad (47)$$

where c_1 and c_2 are constants. The dependence of $\mathbf{\Lambda}_{12}$ is dictated by the tetrahedral site symmetry in the diamond lattice. From Eq. (47), we construct $\mathbf{\Lambda}_{12}^*\mathbf{\Lambda}_{12}$ and find that its symmetry structure in $\mathbf{q}$ space is isomorphic to $\mathbf{\Lambda}_0$. These arguments show that $\sum_q \mathbf{B}_{11}$ is proportional to $\mathbf{I}_3$, since the q_y and q_z axes can be rotated into q_x and the off-diagonal elements vanish by reflection in the q_x, q_y, or q_z plane. Finally, since the upper right and lower left 3×3 blocks of Eq. (43) are identical, $\mathbf{D}_1$ can be expressed in terms of the trace of $[\tau \mathbf{I}_6 - \mathbf{\Lambda}]^{-1}$ or more simply as

$$\mathbf{D}_1 = \mathbf{I}_3 \int_0^{\omega_M} d\omega \, N(\omega)[\tau - \omega^2]^{-1}, \qquad (48)$$

where $N(\omega)$ is the density of vibrational states per unit frequency and ω_M denotes the maximum frequency. The $N(\omega)$ function is normalized to unity, i.e.,

$$\int_0^{\omega_M} d\omega \, N(\omega) = 1. \qquad (49)$$

III. MOMENTUM TRANSFER AND γ-RAY CROSS SECTION FOR AN ISOTOPICALLY SUBSTITUTED NUCLEUS IN GERMANIUM

The momentum transfer and γ-ray cross section of an impurity nucleus of mass, M_I, isotopically substituted into the germanium lattice are studied in this section. In this case, $\Delta \mathbf{F} = 0$ in Eq. (32) and Eq. (31) can now be written as

$$\{\mathbf{G}(\tau)\}_{11} = \mathbf{I}_3(1+\epsilon)\mathfrak{D}(\tau)[1+\tau\epsilon\mathfrak{D}(\tau)]^{-1}, \qquad (50)$$

where

$$\mathfrak{D}(\tau) = \int_0^{\omega_M} d\omega \, N(\omega)[\tau - \omega^2]^{-1} \qquad (51)$$

is the scalar part of Eq. (48). From Eqs. (19) and (50), one obtains

$$\{f_0(\mathbf{\Omega})\}_{11} = \mathbf{I}_3(1/\pi) \lim_{\delta \to 0} \int_0^\infty d\tau f_0(\tau^{1/2})(1+\epsilon)$$

$$\times \text{Im}\mathfrak{D}(\tau')[1+\tau'\epsilon\mathfrak{D}(\tau')]^{-1}, \qquad (52)$$

where $\tau' = \tau - i\delta$. One should note that the contribution to the above integral for $\tau < 0$ vanishes identically for a stable lattice.

A. Behavior of $\mathfrak{D}(\tau)$ Near Real Axis

From Eq. (51), one notes that

$$\mathfrak{D}(\tau - i\delta) = \int_0^{\omega_M} d\omega \, N(\omega) \frac{(\tau - \omega^2)}{[\tau - \omega^2]^2 + \delta^2}$$

$$+ i \int_0^{\omega_M} d\omega \, N(\omega) \frac{\delta}{[\tau - \omega^2]^2 + \delta^2}, \qquad (53)$$

where τ is considered to be real, i.e., $0 \le \tau < \infty$. The density of modes function $N(\omega)$ is proportional to ω^2 for small ω, vanishes at $\omega = \omega_M$, and is continuous over the interval $0 \le \omega \le \omega_M$ for a three-dimensional crystal. Phillips[13] has shown that $N(\omega)$ has a finite number of critical points, ω_c, for which $N(\omega)$ is proportional to $a_1|\omega^2 - \omega_c^2|^{1/2} + a_2$ for ω near ω_c, where a_1 and a_2 are constants.

1. $0 \le \tau \le \tau_M$

When τ lies in the continuum $0 \le \tau \le \tau_M \equiv \omega_M^2$, the real part of $\mathfrak{D}(\tau - i\delta)$ tends to an improper integral independent of δ, while the imaginary part tends to $i\pi N(\tau^{1/2})/(2\tau^{1/2})$ according to the same analysis which

established Eq. (18) as $\delta \to 0$. One can readily show, however, that

$$\lim_{\delta \to 0} \int_0^{\omega_M} d\omega \, N(\omega) \frac{(\tau - \omega^2)}{[\tau - \omega^2]^2 + \delta^2}$$

$$\equiv P \int_0^{\omega_M} d\omega \, N(\omega)[\tau - \omega^2]^{-1}$$

$$\equiv [N(\tau^{1/2})/(2\tau^{1/2})] \ln[(\omega_M + \tau^{1/2})/(\omega_M - \tau^{1/2})]$$

$$- \int_0^{\omega_M} d\omega \left[\frac{N(\omega) - N(\tau^{1/2})}{\omega^2 - \tau} \right], \quad (54)$$

where P denotes the Cauchy principal value of the integral. The analytic character of the last integral can be investigated by subdividing the continuum into regions delineated by the critical points. A detailed investigation of this integral shows that it is continuous for $0 \leq \tau \leq \omega_M^2$ (and bounded) and has discontinuous derivatives at the critical points. Consequently, one can interchange the limiting process, $\delta \to 0$, and the integration process in Eq. (52) over the continuum region $0 \leq \tau \leq \omega_M^2$.

2. $\tau > \omega_M^2$

When τ lies beyond the continuum limit or ω_M^2, the imaginary part of $\mathfrak{D}$ is proportional to δ for small δ. If

$$1 + \tau_L \epsilon \mathfrak{R}(\tau_L) = 0, \quad (55)$$

for $\tau_L > \omega_M^2$, where

$$\mathfrak{R}(\tau) = \int_0^{\omega_M} d\omega \, N(\omega)[\tau - \omega^2]^{-1}, \quad (56)$$

then a *localized* mode occurs and a singular contribution to Eq. (52) may exist. Since

$$\frac{d}{d\tau}\{1 + \tau \epsilon \mathfrak{R}(\tau)\} = -\epsilon \int_0^{\omega_M} d\omega \, N(\omega)\omega^2[\tau - \omega^2]^{-2},$$
$$\tau > \omega_M^2, \quad (57)$$

it is clear that $1 + \tau \epsilon \mathfrak{R}$ is a monotonic function of τ for increasing τ, and consequently, Eq. (55) has at most a single solution. Furthermore, it is necessary that $M_H > M_I$ or

$$-\epsilon \int_0^{\omega_M} d\omega \, N(\omega)[\omega_M^2 - \omega^2]^{-1} \geq 1, \quad (58)$$

in order that a localized mode exist.

B. The Dynamic Response Function, $K(x,\epsilon)$

In order to simplify the notation, we introduce a new frequency scale and transform τ to a new variable

$$\tau^{1/2} = x(\omega_M/x_M), \quad \omega = y(\omega_M/x_M), \quad (59)$$

where $0 \leq x$, $y \leq x_M$ denotes the new continuum. [For germanium, $x_M = 0.895$ which happens to be $\frac{1}{10}$ of the scale used by Phillips.[13] However, for aluminum, we use $x_M = 1$.] With this convention $\tau' \mathfrak{D}(\tau')$, $\tau' = \tau - i\delta$ goes over to $x^2[R(x) + i\pi N(x)/(2x)]$, where

$$R(x) = P \int_0^{x_M} dy \, N(y)[x^2 - y^2]^{-1}, \quad \int_0^{x_M} dy \, N(y) = 1 \quad (60)$$

and

$$N(y) = 0, \quad y \geq x_M. \quad (61)$$

Equation (52) can now be written as

$$\{f_0(\mathbf{\Omega})\}_{11} = \mathbf{I}_3 \int_0^\infty dx \, f_0\left(\frac{\omega_M x}{x_M}\right) K(x,\epsilon), \quad (62)$$

where

$$K(x,\epsilon) = (1+\epsilon)N(x)\{[1 + \epsilon x^2 R(x)]^2 + [\epsilon \pi (x/2)N(x)]^2\}^{-1} + a_L \delta(x - x_L) \quad (63)$$

and a_L is either zero or

$$a_L = (1+\epsilon)\epsilon^{-1}R(x_L)\{[x_L^2 R(x_L)]'\}^{-1}, \quad (64)$$

provided a localized mode exists at $\omega = \omega_L$ or $x = x_L$ given by

$$1 + \epsilon x_L^2 R(x_L) = 0. \quad (65)$$

The first term in Eq. (63) is zero for $x \geq x_M$ and δ denotes Dirac's delta function. The prime appearing in Eq. (64) denotes differentiation with respect to x_L. The contribution to a_L is obtained by expanding $1 + \tau' \epsilon \mathfrak{D}(\tau')$ about $\tau' = \tau_L$ in Eq. (52), and evaluating the integral in the same manner as Eq. (18) was established.

1. Conservation of States Rule

If f_0 is a constant in Eq. (62), we obtain the important result that

$$\int_0^\infty dx \, K(x,\epsilon) \equiv 1. \quad (66)$$

This conservation rule is extremely valuable for purposes of numerical calculations. In fact,

$$a_L = 1 - \int_0^{x_M} dx \, K(x,\epsilon), \quad (67)$$

for all ϵ and any $N(x)$ function obeying the previously outlined requirements.

C. The $g(\mu)$ Function

The $g(\mu)$ function defined by Eqs. (16) and (17) takes the simple form

$$g(\mu) = [p^2 x_M/(2M_I \hbar \omega_M)] \int_0^\infty dx \, K(x,\epsilon)$$

$$\times \{(\cos x\sigma - 1) \coth(x\rho) - i \sin x\sigma\} x^{-1}, \quad (68)$$

where

$$\sigma = (\hbar\omega_M/x_M)\mu; \quad \rho = \hbar\omega_M/(2x_MkT). \qquad (69)$$

1. Lamb-Mössbauer Coefficient, 2W

The resonant fraction, f, of γ rays absorbed, using Lamb's original formalism, is given by $f = \exp(-2W)$, where $2W$ is the Lamb-Mössbauer coefficient defined as the negative of the μ-independent part of Eq. (68). [The factor, f, is commonly called the Debye-Waller factor because of its similarity to the Debye-Waller factor occurring in x-ray scattering theory.[1]] From Eq. (68), one has

$$2W = \chi \int_0^\infty dx \, K(x,\epsilon) x^{-1} \coth(x\rho), \qquad (70)$$

where

$$\chi = [p^2 x_M/(2M_I\hbar\omega_M)]. \qquad (71)$$

2. Resonant Absorption Cross Section when Localized Mode Exists

Kaufman and Lipkin[19] have pointed out that the resonant fraction of γ rays absorbed is the μ-independent part of $e^{g(\mu)}$ and not e^{-2W}. If a localized mode exists, i.e., if $a_L \neq 0$ in Eq. (63), then they argue that $f \neq e^{-2W}$. We note that Eq. (68) can be written as

$$g(\mu) = -2W + \chi \int_0^{x_M} dx \, K(x,\epsilon)$$

$$\times \{\cos(x\sigma) \coth(x\rho) - i \sin(x\sigma)\} x^{-1}$$

$$+ \chi(a_L/x_L)\{\cos(x_L\sigma) \coth(x_L\rho) - i \sin(x_L\sigma)\}. \qquad (72)$$

It is easily shown that the second term tends to zero for large μ and does not contribute to the resonant f. The third term contributes to f since it does not vanish as $\mu \to \infty$, but oscillates and an analysis similar to that given by Kaufman and Lipkin leads to

$$f = e^{-2W_c} e^{-2W_L} I_0\{2[(W_L)^2 - (W_{L0})^2]^{1/2}\}, \qquad (73)$$

where

$$2W_c = \chi \int_0^{x_M} dx \, K(x,\epsilon) x^{-1} \coth(x\rho) \qquad (74)$$

represents the continuum contribution to the Lamb-Mössbauer coefficient, $I_0(x)$ is a Bessel function of order zero having an imaginary argument,

$$2W_L = \chi(a_L/x_L) \coth(x_L\rho), \qquad (75)$$

and

$$2W_{L0} = \chi(a_L/x_L) \qquad (76)$$

is the contribution to the Lamb-Mössbauer coefficient from the localized mode at $T = 0$ or $\rho = \infty$.

It is clear that an enhancement in f occurs, i.e.,

$f > e^{-2W}$, where $2W \equiv 2W_c + 2W_L$, when a localized mode is present, particularly if $2W_L$ is large compared to unity and $2W_c \ll 2W_L$.

D. Numerical Results for the Germanium Lattice

The frequency spectrum for Ge, derived by Phillips,[13] has been used to construct the $R(x)$ function [Eq. (60)], which was calculated from $S(x) = N(x)/(2x)$ by taking $N(x)$ to vary linearly between the tabulated points. [Tables of R and N can be obtained from the authors, if desired.]

One can construct $K(x,\epsilon)$ from $N(x)$ and $R(x)$ for any desired $M_I/M_H = 1 + \epsilon$ from Eq. (63). In Fig. 1, we show the behavior of $K(x,\epsilon)$ for Ge-Sn[119] for which $\epsilon = 0.63$. This dynamic response function can be approximated by three Breit-Wigner resonances. The highest frequency resonance at $x_c = 0.79$ has a long lifetime and has a frequency half-width of $\Delta x = 0.007$. Resonances occur in the continuum when $1 + \epsilon x_c^2 R(x_c) = 0$ and the resonance half-width is Δx given by

$$\Delta x = \pi(x_c/2)N(x_c)|[x_c^2 R(x_c)]'|, \qquad (77)$$

where the prime denotes differentiation with respect to x at $x = x_c$.

In Fig. 2, we have plotted the $2W$ function for a Sn[119] atom in a Ge lattice as a function of temperature using Eq. (70). The Sn[119] recoil energy, $p^2/(2M_I)$, is 26 keV and $\hbar\omega_M = k\theta_M$, where $\theta_M = 372°$K for Ge. It is quite interesting to note that at room temperature $2W$ for an isotopically substituted Sn[119] atom in Ge is almost a factor of 3 times smaller than $2W$ for a Sn[119] atom in a Sn crystal as determined experimentally.[22] We also show two theoretically determined curves for the Sn-Sn[119] for sake of comparison. Both of the curves were derived from the A-S lattice dynamics model[23] with curve A referring to results derived on the basis of elastic constant measurements of Rayne and Chandrasekhar[24] and curve B based on similar measurements of Bömmel and Mason.[25] The fraction of resonantly absorbed γ rays is given by $f = e^{-2W}$, here. One can also determine the total absorption cross section from Eqs. (10) and (68).

[22] A. J. F. Boyle, D. St. P. Bunbury, C. Edwards, and H. E. Hall, Proc. Phys. Soc. (London) A77, 129 (1961).

[23] The theoretical curves shown in Fig. 2 were derived from an application of the A-S lattice dynamics model. See G. W. Lehman, T. Wolfram, and R. E. DeWames, Phys. Rev. 128, 1593 (1962). For a discussion of the lattice dynamics of white tin, see T. Wolfram, G. W. Lehman, and R. E. DeWames, ibid. 129, 2483 (1963). The calculation of the Debye-Waller factor for white tin is given in another paper, see R. E. DeWames, T. Wolfram, and G. W. Lehman ibid. 131, 529 (1963).

[24] J. A. Rayne and B. S. Chandrasekhar, Phys. Rev. 120, 1658 (1960).

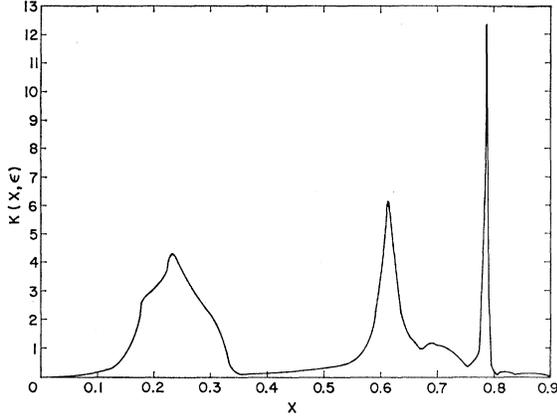[25] W. E. Mason and H. E. Bömmel, J. Acoust. Soc. Am. 28, 930 (1956).

FIG. 1. Dynamic response function for Sn^{119} isotopically substituted in germanium.

IV. DYNAMICAL BEHAVIOR OF AN ISOLATED IMPURITY ATOM SUBSTITUTED INTO ALUMINUM WITH ARBITRARY CHANGES IN FIRST-NEIGHBOR FORCE CONSTANTS

In Sec. II, we established a simple prescription for calculating $\{f_0(\mathbf{\Omega})\}_{11}$ in terms of the $\mathbf{A}_{11}$ matrix, which depends upon $\mathbf{D}_{z+1}$ and $\Delta \mathbf{F}/M_H$ but is independent of $\epsilon+1=M_I/M_H$. In this section, we express $\mathbf{A}_{11}$ for the case of arbitrary nearest neighbor changes in $\mathbf{F}_H$ for a face-centered cubic lattice in terms of the matrix elements of a symmetry adapted Green's function. Physically, the impurity atom is coupled to the host-lattice atoms in the fashion of a giant molecule. Only those modes which transform like (x,y,z) interact. Clearly, $\Delta \mathbf{F}$ transforms occurring to the cubic point group and we have already shown that $\mathbf{D}_{z+1}$ does likewise. Consequently, it is most convenient to construct the $\mathbf{D}_{z+1}$ matrix using the molecular vibration symmetry coordinates associated with the impurity atom and the 12 nearest neighbor atoms. A simple group theoretical calculation shows that only 3 of the 36 symmetry coordinates associated with the 12 nearest neighbor atoms couple to the x component of the impurity atom coordinate. Of course, the y and z motion is degenerate with that in the x direction and need not be considered.

A. Symmetry Adapted Green's Function for Face-Centered Cubic Lattice

In order to proceed further, it is necessary to work out the symmetry coordinates which transform like the x-direction motion of the impurity atom. If the impurity atom is located at $\mathbf{R}_1=(0,0,0)$, then the equilibrium coordinates of the 12 nearest neighbor atoms can be denoted by $\mathbf{R}_2=(0,1,1)$, $\mathbf{R}_3=(0,-1,1)$, $\mathbf{R}_4=(0,-1,-1)$, $\mathbf{R}_5=(0,1,-1)$, $\mathbf{R}_6=(1,0,1)$, $\mathbf{R}_7=(1,0,-1)$, $\mathbf{R}_8=(-1,0,-1)$, $\mathbf{R}_9=(-1,0,1)$, $\mathbf{R}_{10}=(1,1,0)$, $\mathbf{R}_{11}=(-1,1,0)$, $\mathbf{R}_{12}=(-1,-1,0)$, $\mathbf{R}_{13}=(1,-1,0)$, where the unit of length has been chosen to be $a/2$, half of cube edge.

If $\Delta\mathbf{x}_j=(\Delta x_j,0,0)$, $\Delta\mathbf{y}_j=(0,\Delta y,0)$, and $\Delta\mathbf{z}_j=(0,0,\Delta z_j)$

denote unit-vector displacements of the jth atom in the x, y, and z directions, respectively, then one can easily show by group theory that the 4 symmetry coordinates transforming irreducibly as x are

$$\varphi_1 = \Delta\mathbf{x}_1,$$

$$\varphi_2 = (12)^{-1/2} \sum_{n=2}^{13} \Delta\mathbf{x}_n,$$

$$\varphi_3 = (24)^{-1/2}\Big[2\sum_{n=2}^{5} \Delta\mathbf{x}_n - \sum_{n=6}^{13} \Delta\mathbf{x}_n\Big], \tag{78}$$

$$\varphi_4 = -(8)^{-1/2}\sum_{n=6}^{9}(-1)^n[\Delta\mathbf{z}_n + \Delta\mathbf{y}_{n+4}].$$

Here, φ_1 denotes a unit displacement of the impurity atom in the x direction, while φ_2 denotes a unit displacement in the same direction of the 12 nearest neighbor atoms rigidly locked together. If isotropic restoring forces are assumed, as in the case of Visscher's calculations,[12] then the x, y, and z motion of the entire system decouples and φ_1 and φ_2 completely specify the coupling of the impurity atom to the nearest neighbor shell regarding motion in the x direction. When tensor restoring forces are involved, then φ_3 and φ_4 must be included. The symmetry coordinate φ_3 involves an optic-type motion in the x direction in which the 8 atoms in the x-y and x-z planes move in phase with each other and out of phase with the 4 atoms lying in the y-z plane. The rigid y-z plane motion has an amplitude which is twice that of the rigid x-y, x-z motion and, hence, φ_3 is orthogonal to φ_2. The φ_4 motion is likewise pure optic with *no* displacement in the x direction. This motion is most easily visualized as a distortion of a cube in which the two cube faces perpendicular to the x axis preserve the symmetry of a square with one face expanding while the other face contracts, the amplitude of the motion of the 8 atoms involved is the same.

A complete description of the vibrational modes for an impurity atom in a face-centered cubic lattice with nearest neighbor changes in force constants requires 39 symmetry coordinates. As previously noted, only 4 of these are required for a complete study of the Mössbauer effect. However, if one were interested in computing the thermodynamic properties of our system, it would be necessary to determine the other modes which are not degenerate with Eq. (78). We shall discuss this problem further in the next section of this paper.

Our final task is to construct the $\{\mathbf{G}(\tau)\}_{11}$ matrix from $\mathbf{A}_{11}$ which can be written, according to symmetry arguments given previously, as $\mathbf{A}_{11}=C_x(\tau)\mathbf{I}_3$, where $C_x(\tau)$ denotes the (1,1) diagonal element of the $\mathbf{A}$ supermatrix associated with the x coordinate of the impurity atom, i.e., the φ_1 symmetry coordinate. From Eqs. (34)

$$\mathbf{A} = [\mathbf{I}_{39} - \mathbf{d}(\Delta\mathbf{F}/M_H)]^{-1}\mathbf{d}, \tag{79}$$

where $\mathbf{d}$ is a 39×39 matrix, whose 3×3 supermatrix elements are defined by Eq. (35). We now establish that the (1,1) element of $\mathbf{A}$ is simply the (1,1) element of a 4×4 matrix whose elements are constructed from Eq. (79) in a basis using the symmetry coordinates defined by Eq. (78). Our assertion is physically obvious; however, for completeness we establish the result mathematically. Let ζ be a matrix whose elements are

$$\zeta_{11}=\zeta, \quad \zeta_{ij}=0, \quad (i,j)\neq(1,1), \tag{80}$$

and for brevity put

$$\mathbf{C}=\Delta\mathbf{F}/M_H \tag{81}$$

and observe that

$$\{(\partial/\partial\zeta)\ln\det[\mathbf{I}-\mathbf{dC}+\mathbf{d}\zeta]\}_{\zeta=0}$$
$$=\{(\partial/\partial\zeta)\ln\det[\mathbf{I}+(\mathbf{I}-\mathbf{dC})^{-1}\mathbf{d}\zeta]\}_{\zeta=0}$$
$$=\{(\partial/\partial\zeta)\operatorname{Tr}\ln[\mathbf{I}+(\mathbf{I}-\mathbf{dC})^{-1}\mathbf{d}\zeta]\}_{\zeta=0}$$
$$\equiv([\mathbf{I}-\mathbf{dC}]^{-1}\mathbf{d})_{11}, \tag{82}$$

where ln denotes natural logarithm, det denotes determinant, and Tr denotes trace operation. Equation (82) holds for arbitrary $\mathbf{d}$ and $\mathbf{C}$ as long as $\mathbf{I}-\mathbf{dC}$ is nonsingular which is the case in this paper. We have used det $(\mathbf{AB})=\det(\mathbf{A})\det(\mathbf{B})$ and $\ln\det(\mathbf{A})\equiv\operatorname{Tr}\ln(\mathbf{A})$ in Eq. (82). Next, let $\mathbf{U}$ be a unitary matrix transformation relating the symmetry coordinate φ_j's with the atomic displacement vectors $\Delta\mathbf{x}_n$, $\Delta\mathbf{y}_n$, and $\Delta\mathbf{z}_n$. In Eq. (82), let $\mathbf{d}_T=\mathbf{U}^{-1}\mathbf{dU}$, and note that

$$\det[\mathbf{I}-\mathbf{dC}+\mathbf{d}\zeta]$$
$$\equiv\det[\mathbf{I}-\mathbf{d}_T\mathbf{C}_T]\det[\mathbf{I}+(\mathbf{I}-\mathbf{d}_T\mathbf{C}_T)^{-1}\mathbf{d}_T\zeta],$$

since $\zeta_T=\zeta$. The 39×39 matrix in the second determinant can be written as a 4×4 block whose elements are associated with the φ_j's of Eq. (78) and a 35×35 matrix involving all other symmetry coordinates. We now denote the 4×4 block of the transformed $\mathbf{d}$ and $\mathbf{C}$ matrices by $\mathbf{d}^T$ and $\mathbf{C}^T$ and observe that

$$\det[\mathbf{I}+(\mathbf{I}-\mathbf{d}_T\mathbf{C}_T)^{-1}\mathbf{d}_T\zeta]=\det[\mathbf{I}_4+(\mathbf{I}_4-\mathbf{d}^T\mathbf{C}^T)^{-1}\mathbf{d}^T\zeta]$$
$$=1+([\mathbf{I}_4-\mathbf{d}^T\mathbf{C}^T]^{-1}\mathbf{d}^T)_{11}\zeta. \tag{83}$$

Using the procedure shown in Eq. (82) and the relation given by Eq. (81), we obtain our final result

$$\mathbf{A}_{11}=C_x(\tau)\mathbf{I}_3, \tag{84}$$

where

$$C_x(\tau)=([\mathbf{I}_4-\mathbf{d}^T(\Delta\mathbf{F}^T)M_H^{-1}]^{-1}\mathbf{d}^T)_{11}. \tag{85}$$

1. Construction of $\mathbf{d}^T$ in Terms of Symmetry Adapted Functions

The matrix elements of $\mathbf{d}^T$, denoted by $\mathfrak{D}_{jk}$, are easily constructed by noting the form of Eq. (35), In fact,

$$\mathfrak{D}_{jk}=N^{-1}\sum_{\mathbf{q}}(\psi_j,[\tau\mathbf{I}_3-\mathbf{\Lambda}(\mathbf{q})]^{-1}\psi_k), \tag{86}$$

where $(\mathbf{a},\mathbf{b})$ denotes an ordinary inner product between $\mathbf{a}$ and $\mathbf{b}$. The ψ_j's are 3-component vectors constructed from the φ_j's by replacing the row vector representation
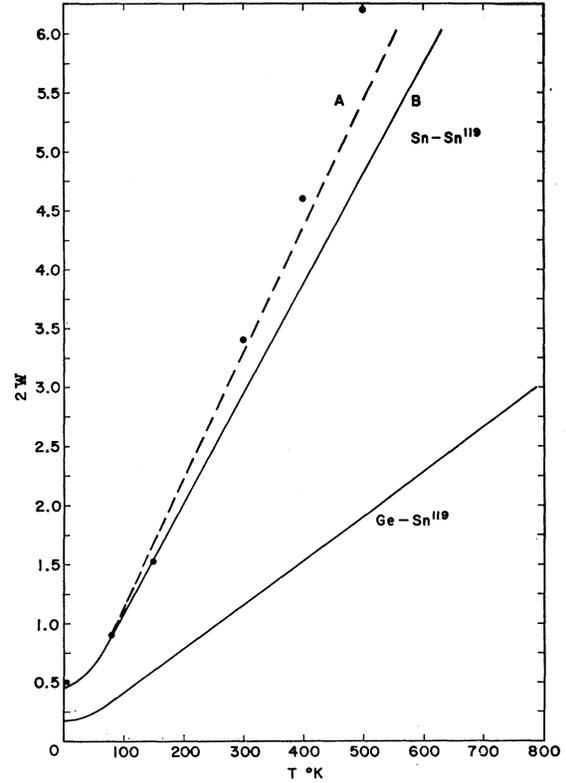

FIG. 2. Lamb-Mössbauer coefficient, $2W$, for Sn^{119} isotopically substituted in germanium as a function of temperature. The other curves refer to Sn^{119} in natural white tin and are included for sake of comparison. [See text for labeling.]

of $\Delta\mathbf{x}_n$ by (100) $\exp(-i\mathbf{q}\,\mathbf{R}_n)$ and similar representations of $\Delta\mathbf{y}_n$ and $\Delta\mathbf{z}_n$. From Eq. (78) and the definition of the $\mathbf{R}_n$'s ,one obtains

$$\psi_1=\begin{bmatrix}1\\0\\0\end{bmatrix}, \quad \psi_2=(\tfrac{4}{3})^{1/2}[C_xC_y+C_yC_z+C_zC_x]\psi_1,$$

$$\psi_3=(\tfrac{2}{3})^{1/2}[2C_yC_z-C_x(C_y+C_z)]\psi_1, \tag{87}$$

$$\psi_4=2^{1/2}S_x\begin{bmatrix}0\\S_y\\S_z\end{bmatrix},$$

where $C_x=\cos(aq_x/2)$, $S_x=\sin(aq_x/2)$, $x=x, y, z$.

B. Numerical Results for Symmetry Adapted Green's Function for Aluminum

Since

$$\mathbf{\Lambda}\xi_p=[\omega_p(\mathbf{q})]^2\xi_p, \tag{88}$$

where $\omega_p(\mathbf{q})$ is the eigenfrequency associated with the pth polarization vector ξ_p, we can write

$$\mathfrak{D}_{jk}=\int_0^{\omega_M}d\omega[\tau-\omega^2]^{-1}N_{jk}(\omega), \tag{89}$$

where

$$N_{jk}(\omega)=v^{-1}\int d\mathbf{q}\sum_{p=1}^{3}\delta(\omega-[\omega_p(\mathbf{q})]^2)Q_{jp}Q_{kp},\quad(90)$$

and

$$Q_{jk}=(\boldsymbol{\psi}_j,\boldsymbol{\xi}_p).\quad(91)$$

The integration in Eq. (90) is to be taken over the reduced Brillouin zone having volume v.

From Eqs. (90) and (91),

$$\int_0^{\omega_M}d\omega\,N_{jk}(\omega)=v^{-1}\int d\mathbf{q}\,(\boldsymbol{\psi}_j,\boldsymbol{\psi}_k)\equiv\delta_{jk},\quad(92)$$

as can be established from Eq. (87) and the orthogonality relations

$$N^{-1}\sum_{\mathbf{q}}\exp[i\mathbf{q}\cdot(\mathbf{R}_j-\mathbf{R}_k)]=\delta_{jk}.\quad(93)$$

The element $N_{11}(\omega)$ is the ordinary density of modes function for a monatomic face-centered cubic crystal. We refer to N_{jk} as density-of-modes matrix elements and note that critical points occur in these functions at frequencies which are identical to the critical points for $N_{11}(\omega)$.

1. Numerical Values of $R_{ij}(x)$ and $N_{ij}(x)$ for Aluminum

According to the detailed analysis of the previous section on the Green's function for Ge, we see that the dynamic response function given by Eq. (63) can be used here provided $R(x)$ and $N(x)$ are replaced by $R_{\text{eff}}(x)$ and $N_{\text{eff}}(x)$, respectively. We find

$$R_{\text{eff}}(x)=\text{Re}([\mathbf{I}_4-\mathbf{D}\boldsymbol{\kappa}]^{-1}\mathbf{D})_{11}\quad(94)$$

and

$$N_{\text{eff}}(x)=(x/\pi)\,\text{Im}([\mathbf{I}_4-\mathbf{D}\boldsymbol{\kappa}]^{-1}\mathbf{D})_{11},\quad(95)$$

where

$$\mathbf{D}=\mathbf{R}+i\pi\mathbf{S},\quad(96)$$

$$R(x)=\int_0^1 dy\,N(y)[x^2-y^2]^{-1},\quad S=\frac{N}{2x},\quad(97)$$

and

$$\boldsymbol{\kappa}=\Delta\mathbf{F}^T/(M_H\omega_M{}^2).\quad(98)$$

We have used Walker's atomic-force constants[15] derived from diffuse thermal x-ray scattering data on aluminum to calculate the 4×4 $\mathbf{N}$ matrix whose elements are defined by Eq. (90). A mesh of 45 000 points was used over 1/48 of the Brillouin zone and N_{jk} was computed by suitable symmetrization of $Q_{jp}Q_{kp}$. The delta function in Eq. (90) was replaced by a step func-

tion of width $\Delta\omega=0.005\omega_M$ and height $(1/\Delta\omega)$. The resulting histogram indicated that more points should have been taken for our $\Delta\omega$ used. The ten histograms for N_{jk} were carefully examined by plotting and cross plotting. Our N_{11} function agrees quite satisfactorily with Walker's density of modes but has more structure. We were able to choose 88 ω/ω_M points which allowed us to calculate N_{jk} by linear or quadratic interpolation for $0\le\omega/\omega_M\le1$. The final N_{jk} curves satisfied the orthonormality rule, Eq. (92) to about 1% in the worst case. This error was actually introduced by our smoothing technique as our histograms satisfied Eq. (92) to better than 0.2% in all cases. [Tables of N_{jk} and R_{jk} are available from the authors upon request.]

C. Construction of $\Delta\mathbf{F}^T$ Matrix

One of the simplest ways to construct a $\Delta\mathbf{F}^T$ matrix is by examining the A-S lattice dynamics model which is a special case of the generalized tensor force model[23] used by Walker for aluminum.[15] In fact, Walker's force constants for aluminum are essentially axially symmetric. According to this model, the 3×3 matrix which describes the interaction between the ith and jth atom is

$$\{\mathbf{F}\}_{ij}=\delta_{ij}\sum_{s=1}^{N}\mathbf{k}_{sj}-\mathbf{k}_{ij},\quad(99)$$

where

$$\mathbf{k}_{ij}=C_{SB}(r_{ij})\begin{bmatrix}l^2, & lm, & ln\\ lm, & m^2, & mn\\ ln, & mn, & n^2\end{bmatrix}+C_B(r_{ij})\mathbf{I}_3,\quad(100)$$

with C_{SB} referring to the difference between a stretching and a bending force constant and C_B denoting a bending force constant. The vector $\mathbf{r}_j=(x_j,y_j,z_j)$ denotes the equilibrium position of the jth atom, $r_{jk}=|\mathbf{r}_{jk}|$, and (l,m,n) is $(r_{ij})^{-1}(x_{ij},y_{ij},z_{ij})$. Equations (100) and (101) hold for an arbitrary arrangement of the N atoms.

The $\{\Delta\mathbf{F}\}_{ij}$ matrices for the A-S model are obtained from the above equations by replacing the $\mathbf{k}_{ij}$'s by $\Delta\mathbf{k}_{ij}$, and C_{SB} and C_B by ΔC_{SB} and ΔC_B, respectively. When the perturbation is restricted to the nearest neighbor shell of the impurity atom in a face-centered cubic crystal, it is easy to construct $\Delta\mathbf{k}_{ij}$ for the generalized tensor force model used by Walker.[15] In fact, one need only multiply the off-diagonal terms in Eq. (101) by a scale factor, thereby introducing a third force constant for the first-neighbor shell. In Walker's notation, the change in $\mathbf{k}_{1j}$ associated with the impurity atom nearest neighbor coupling is

$$\Delta\mathbf{k}_{1j}=\begin{bmatrix}[2\Delta\alpha_1 l^2+\Delta\beta_1(m^2+n^2)], & 2\Delta\gamma_1 lm, & 2\Delta\gamma_1 ln\\ 2\Delta\gamma_1 lm, & [2\Delta\alpha_1 m^2+\Delta\beta_1(n^2+l^2)], & 2\Delta\gamma_1 mn\\ 2\Delta\gamma_1 ln, & 2\Delta\gamma_1 mn, & [2\Delta\alpha_1 n^2+\Delta\beta_1(l^2+m^2)]\end{bmatrix},\quad(101)$$

where l, m, and n denote the direction cosines between an impurity atom and a nearest neighbor atom. It is further assumed in this paper that $\Delta \mathbf{k}_{ij}=0$ when i or $j \neq 1$. These perturbations are easily included but are not warranted in the present work, unless higher neighbor interactions are included. The correlation between the A-S force-constant changes and the generalized tensor force model changes are[23]

$$\Delta \alpha_1 = \Delta C_B + (\Delta C_{SB}/2),$$

$$\Delta \beta_1 = \Delta C_B, \qquad (102)$$

$$\Delta \gamma_1 = \Delta \alpha_1 - \Delta \beta_1 = \Delta C_{SB}/2.$$

The force constants for pure aluminum are shown in Table I.

1. Construction of the κ Matrix

The next task is to construct the 4×4 matrix, κ, defined by Eq. (98) using the φ_j's of Eq. (78) as basis vectors. The calculations are lengthy but straightforward and we find that the matrix elements $\kappa_{ij}=\kappa_{ji}$ of κ can be written as

$$\kappa_{11}=12\eta_1, \quad \kappa_{12}=(12)^{1/2}\eta_1, \quad \kappa_{13}=(12)^{1/2}\eta_2,$$

$$\kappa_{14}=(12)^{1/2}\eta_3, \quad \kappa_{22}=\eta_1, \quad \kappa_{23}=-\eta_2, \quad \kappa_{24}=-\eta_3, \qquad (103)$$

$$\kappa_{33}=\eta_4, \quad \kappa_{34}=\eta_5, \quad \kappa_{44}=\eta_6,$$

where

$$M_H \omega_M^2 \eta_1 = 4(\Delta \alpha_1 + \Delta \beta_1)/3,$$

$$M_H \omega_M^2 \eta_2 = (2/9)^{1/2}(2\Delta \alpha_1 - \Delta \beta_1),$$

$$M_H \omega_M^2 \eta_3 = (8/3)^{1/2}\Delta \gamma_1,$$

$$M_H \omega_M^2 \eta_4 = (2\Delta \alpha_1 + 5\Delta \beta_1)/3, \qquad (104)$$

$$M_H \omega_M^2 \eta_5 = (4/3)^{1/2}\Delta \gamma_1,$$

$$M_H \omega_M^2 \eta_6 = 2\Delta \alpha_1 + \Delta \beta_1.$$

2. Isotropic Changes in κ

If $\Delta \beta_1 = 2\Delta \alpha_1$ and $\Delta \gamma_1 = 0$, $\Delta \mathbf{k}_{1j} = 2\Delta \alpha_1 \mathbf{I}_3$, the perturbation in restoring force acting between the impurity atom and the nearest neighbors is independent of

direction or isotropic. In this case, $\eta_2 = \eta_3 = \eta_5 = 0$ and $\eta_4 = \eta_6$ and

$$\kappa = [4\Delta \alpha_1/(M_H \omega_M^2)] \begin{bmatrix} 12, & -(12)^{1/2}, & 0 & 0 \\ -(12)^{1/2}, & 1, & 0 & 0 \\ 0, & 0, & 1 & 0 \\ 0, & 0, & 0 & 1 \end{bmatrix}. \qquad (105)$$

D. Numerical Results for Al-Fe[57]

Experimental Mössbauer studies on the Al-Fe[57] system are currently being carried out at our laboratory. However, at the present writing, no experimental data are available. Consequently, we have calculated the response function, K, for several sets of $\Delta \alpha_1$, $\Delta \beta_1$, and $\Delta \gamma_1$, with $\epsilon = 1.1111$. We recall that K is given by Eqs. (63), where $R(x)$ and $N(x)$ are replaced by $R_{\text{eff}}(x)$ and $N_{\text{eff}}(x)$ defined by Eqs. (94) and (95). In these equations, the matrix elements of $\mathbf{R}(x)$ and $\mathbf{S}(x)$ are those appropriate to aluminum, and the matrix elements of the reduced force-constant matrix, κ, are given by Eqs. (103) and (104).

TABLE I. Atomic force constants for aluminum (in units of 10^3 dyn/cm).

Force constant	Walker's value	A-S value
α_1	8.45	8.45
β_1	−0.93	−0.9
γ_1	10.67	9.35
α_2	2.14	2.0
β_2	0.40	−1.0
α_3	0.27	0
β_3	−0.31	0
γ_3	0.10	0
δ_3	−0.19	0

The numerical calculations reported here were carried out on the IBM 7090 electronic digital computer using Fortran programming. These programs were constructed for the general case of arbitrary ϵ and κ. The frequency dependence of K and the temperature dependence of $2W$ and the mean square velocity of the impurity atom, $(v_I^2)_{\text{av}}$ can be obtained in less than 5 min for a particular choice of ϵ, $\Delta \alpha_1$, $\Delta \beta_1$, and $\Delta \gamma_1$.

TABLE II. $2W = [p^2/(2M_I \hbar \omega_M)]\langle 1/x \rangle$ and $M_I (v_I^2)_{\text{av}} = (3k\theta_M/2)\langle x \rangle$ as functions of temperature for various sets of force-constant changes, in units of 10^3 dyn/cm, for Fe[57] in Al. Here, $\hbar \omega_M = k\theta_M$ and $\omega_M = 5.94 \times 10^{13}$ rad/sec. $\langle x^n \rangle$ is defined in text.

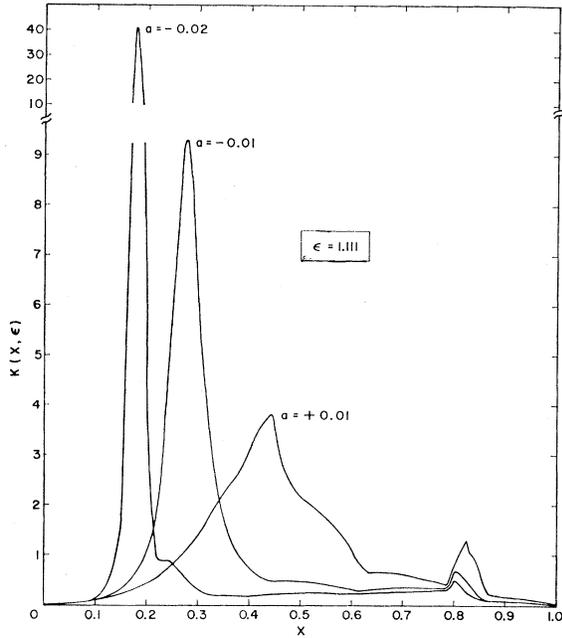| $\Delta \alpha_1$	−1.0		−0.8		−0.4		0		0.4		−2.0		2.0		4.0	
$\Delta \beta_1$	−2.0		−1.6		−0.8		0		0.8		0		0		0	
$\Delta \gamma_1$	0		0		0		0		0		−2.0		2.0		4.0	
T/θ_M	$\langle 1/x \rangle$	$\langle x \rangle$	$\langle 1/x \rangle$	$\langle x \rangle$	$\langle 1/x \rangle$	$\langle x \rangle$	$\langle 1/x \rangle$	$\langle x \rangle$	$\langle 1/x \rangle$	$\langle x \rangle$	$\langle 1/x \rangle$	$\langle x \rangle$	$\langle 1/x \rangle$	$\langle x \rangle$	$\langle 1/x \rangle$	$\langle x \rangle$
0	9.73	0.16	5.07	0.24	3.37	0.34	2.72	0.42	2.40	0.48	3.56	0.30	2.36	0.50	2.15	0.58
0.1	21.9	0.27	7.21	0.30	4.02	0.38	3.03	0.44	2.71	0.49	4.32	0.34	2.69	0.52	2.46	0.59
0.2	41.5	0.45	12.2	0.46	6.01	0.51	4.18	0.55	3.66	0.59	6.53	0.48	3.66	0.61	3.28	0.67
1.0	203.2	2.05	57.2	2.01	26.3	2.02	17.2	2.03	14.7	2.04	28.8	2.02	14.7	2.05	12.9	2.06
2.0	...	...	...	...	...	...	...	...	...	...	57.4	4.01	29.2	4.02	25.6	4.03
10.0	2030	20.42	570.0	19.94	261.0	20.00	170.6	19.97	144.9	20.01	286.7	20.00	145.5	20.00	127.4	20.01

FIG. 3. Dynamic response function for Fe^{57} in aluminum for various isotropic changes in nearest neighbor force constants. (Cf. Table II.)

1. Typical Response Functions for Al-Fe^{57}

The frequency dependence of typical dynamic response functions associated with isotropic changes in κ [cf., Eq. (106)] are shown in Fig. 3 for three choices of a, where $a=4\Delta\alpha_1/(M_H\omega_M^2)$. For aluminum, $\omega_M=5.9\times10^{13}$ rad/sec, $M_H=0.45\times10^{-22}$ G so that $\Delta\alpha_1=(40\times10^3)a$ dyn/cm, $\Delta\beta_1=2\Delta\alpha_1$, $\Delta\gamma_1=0$. These curves show that one can have quite localized K functions corresponding to continuum resonances of the type discussed by Brout and Visscher,[10] Visscher,[12] and Lehman and DeWames.[11]

The frequency dependence of the K function was also calculated for several sets of pure bond-stretching changes in force constants for which $\Delta\alpha_1=\Delta\gamma_1$ and $\Delta\beta_1=0$ but will not be presented here.

2. 2W and $(v_I^2)_{av}$ for Al-Fe^{57}

Typical numerical results are presented in Table II showing the temperature dependence of the Lamb-Mössbauer coefficient, $2W$, and the mean square velocity of the impurity atom, $(v_I^2)_{av}$, for several sets of force-constant changes when Fe^{57} is substituted into the aluminum lattice. These quantities are given by

$$2W = [p^2/(2M_I\hbar\omega_M)]\langle 1/x\rangle \qquad (106)$$

and

$$M_I(v^2)_{av} = (3k\theta_M/2)\langle x\rangle, \qquad (107)$$

where

$$\langle x^n\rangle = \int_0^\infty dx\, K(x,\epsilon)x^n \coth\left(\frac{x\theta_M}{2T}\right) \qquad (108)$$

and $k\theta_M=\hbar\omega_M$, with $\theta_M=440°$K for aluminum. Equation (106) follows from Eq. (70). The derivation of Eq. (107) follows a pattern similar to that used in obtaining $2W$. Note that $\langle x\rangle \to 2T/\theta_M$ as $T\to\infty$ by Eq. (66) so that $M_I(v^2)_{av} \to 3kT$ as required, i.e., when $T\to\infty$, the average kinetic energy of the impurity atom is simply $\frac{1}{2}kT$ per degree of freedom in momentum space independent of the binding forces holding the atoms together. The fifth column of Table II corresponds to an atom isotopically substituted into the aluminum lattice. It is important to note that changes in β_1 have a quite pronounced effect on $2W$ and $(v^2)_{av}$, the mean square velocity of the Fe^{57} atom, even though α_1 and γ_1 are nearly 10 times larger than β_1 according to Table I. The recoil energy, $p^2/2M_I$, for Fe^{57} is 0.0018 eV and $k\theta_M=0.037$ so that $2W=0.049\langle 1/x\rangle$. Hence, the fraction, f, of γ rays resonantly absorbed by Fe^{57} nuclei isotopically substituted into aluminum is $f=0.43$ at $440°$K and $f=0.88$ at $0°$K. If $\Delta\beta_1=2\Delta\alpha_1=-2\times10^3$ dyn/cm and $\Delta\gamma_1=0$, column 2 of Table II shows that $f=0.00005$ at $440°$K and $f=0.69$ at $0°$K. On the other hand, the last column of this table shows that $f=0.63$ at $440°$K and $f=0.9$ at $0°$K when $\Delta\alpha_1=\Delta\gamma_1=4\times10^{13}$ dyn/cm and $\Delta\beta_1=0$. The other columns of Table II show results intermediate to these two extremes.

3. High-Temperature Form for 2W

We now show that $2W$ can be expressed quite simply when $T/\theta_M\gtrsim1$. From Eqs. (6) and (20), one notes that $\{\mathbf{G}(\tau=0)\}_{11}(\omega_M)^2 = -\{\mathbf{\Omega}^{-2}\}_{11}$ for a completed arbitrary set of atoms coupled together harmonically. On the other hand, for an isolated impurity in a monatomic cubic lattice, Eqs. (31), (84), (85), (94), and (96) show that

$$\{\mathbf{G}(\tau=0)\}_{11}(\omega_M)^2 = (1+\epsilon)R_{eff}(0)\mathbf{I}_3, \qquad (109)$$

where

$$R_{eff}(0) = ([\mathbf{I}_4-\mathbf{R}(0)\kappa]^{-1}\mathbf{R}(0))_{11}, \qquad (110)$$

with

$$\mathbf{R}(0) = -\int_0^1 dy\, \mathbf{N}(y)y^{-2}. \qquad (111)$$

Consequently, using Eqs. (16), (17), (70), and (106) and the above results it can be shown that

$$\langle 1/x\rangle \cong -(2T/\theta_M)(1+\epsilon)([\mathbf{I}_4-\mathbf{R}(0)\kappa]^{-1}\mathbf{R}(0))_{11}, \qquad (112)$$

for large T/θ_M. Since $1+\epsilon=M_I/M_H$, it follows that $2W$ is independent of the mass of the impurity atom for T/θ_M large. This fact is well known physically. From Eq. (110), we obtain the relation

$$\int_0^\infty dx\, x^{-2}K(x,\epsilon)$$
$$= -(1+\epsilon)([\mathbf{I}_4-\mathbf{R}(0)\kappa]^{-1}\mathbf{R}(0))_{11}, \qquad (113)$$

which holds for all ϵ, κ, and $\mathbf{N}$. This relation also provides a very valuable check for computational purposes.

An examination of Table II shows that $\langle 1/x \rangle$ is practically linear with T for $T/\theta_M \geq 1$, so that Eq. (114) provides us with a useful tool. Furthermore, one should note that the matrix elements of $R(0)$ can be obtained from

$$[\mathbf{R}(0)]_{jk} = -N^{-1} \sum_{\mathbf{q}} \sum_{p=1}^{3} [\omega_p(\mathbf{q})/\omega_M]^{-2}$$
$$\times (\boldsymbol{\psi}_j, \boldsymbol{\xi}_p)(\boldsymbol{\psi}_k, \boldsymbol{\xi}_p), \quad (114)$$

by combining Eqs. (90) and (111). Our experience shows that one can evaluate these sums quite accurately by using no more than 1000 points in 1/48 of the Brillouin zone, thereby skipping the troublesome problem of constructing $\mathbf{N}(x)$.

One can easily work out Eq. (115) analytically, if $R(0)$ is known. For aluminum, we find, for an isotropic κ [cf., Eq. (106)], that

$$\int_0^\infty dx\, x^{-2} K(x,\epsilon) = 4.2950(1+\epsilon) J_1(a)[J_2(a)]^{-1}, \quad (115)$$

where

$$J_1(a) = 1 + 14.016a + 47.79a^2 + 47.38a^3,$$
$$J_2(a) = 1 + 41.648a + 171.37a^2 + 184.39a^3, \quad (116)$$

and $a = 2.5 \times 10^{-5} \Delta\alpha_1$. The numerical coefficient on the right side in Eq. (115) is simply $-R_{11}(0)$. It follows from Eqs. (106), (108), and (115) that

$$\langle 1/x \rangle \rightarrow 8.590(1+\epsilon) J_1(a)[J_2(a)]^{-1}(T/\theta_M), \quad (117)$$

at high temperatures for isotropic κ. Table II shows that the above result is quite accurate for $T/\theta_M \geq 1$ for the cases shown in columns 2–5 inclusive. One can also derive a high-temperature result for $\langle 1/x \rangle$ for the case of arbitrary κ, but such a formula is a bit unwieldy and will not be given in this paper.

E. Qualitative Results for Cu-Fe⁵⁷ and Pt-Fe⁵⁷

Since Cu-Fe[57] and Pt-Fe[57] are used extensively as Mössbauer sources, we felt that it was worthwhile to carry out quantitative studies of the temperature dependence of $2W$ and $(v_I^2)_{av}$ using the symmetry adapted Green's function obtained for the aluminum lattice with an appropriate choice of ω_M. Our experimental colleagues inform us that no reliable data exists on these two systems so that we have used the isotropic κ to study the behavior of $2W$.

1. Cu-Fe⁵⁷ ($\epsilon = -0.1$)

For these cases, no bound mode appears for the calculations carried out and the temperature dependence of $\langle 1/x \rangle$ is shown in Fig. 4 for the isotropic κ case when $a = -0.01$, 0, and 0.01. The Lamb-Mössbauer coefficient, $2W$, is given by Eq. (108) with $\omega_M = 4.4 \times 10^{13}$ rad/sec appropriate to Cu.
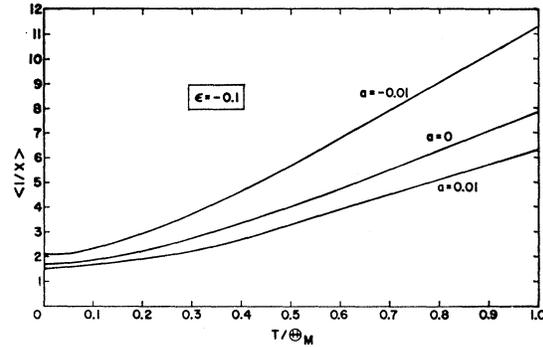

FIG. 4. Relative mean-square displacement, $\langle 1/x \rangle$, as a function of T/θ_M for Fe[57] in copper for various isotropic changes in nearest neighbor force constants. $\theta_M \cong 335°K$.

2. Pt-Fe⁵⁷ ($\epsilon = -0.7$)

For this case, $\langle 1/x \rangle$ is plotted in Fig. 5 for $a = -0.02$, -0.01, 0, 0.01, and $a = \infty$ as a function of T/θ_M. For Pt, we estimate $\omega_M = 3.0 \times 10^{13}$ rad/sec and $\theta_M = 225°K$ from heat-capacity data. The case $a = \infty$ corresponds to the case in which the 12 nearest neighbor atoms of the impurity atom are rigidly coupled to the impurity atom.

In all of these cases, a triply degenerate localized mode appears at a frequency determined by solving Eq. (65), where $R(x_L)$ is replaced by $R_{e^{-f}}(x_L)$ given by Eq. (95). The position, x_L, and the strength, a_L, of the localized modes are presented in Table III along with b_0, b_1, and b_2, where

$$b_n = \int_0^1 dx\, K x^{-n} \quad (118)$$

denotes x^{-n} averaged over the continuum response function. The conservation-of-states theorem, Eq. (66), shows that

$$a_L + b_0 = 1. \quad (119)$$

Equations (63) and (115) give us

$$(x_L)^{-2} a_L + b_2 = -(1+\epsilon)([\mathbf{I}_4 - \mathbf{R}(0)\boldsymbol{\kappa}]^{-1}\mathbf{R}(0))_{11}. \quad (120)$$

The above two equations allow us to determine a_L and x_L if b_0, b_2, and the expression on the right-hand side of Eq. (120) are known. Conversely, if a_L and x_L are

TABLE III. Frequency, $x_L = \omega_L/\omega_M$, and strength, a_L, of a localized mode appropriate to Pt-Fe[57], $\epsilon = -0.7$, for various isotropic force-constant changes $\Delta\beta_1 = 2\Delta\alpha_1$, $\Delta\gamma_1 = 0$, where $a = 4\Delta\alpha_1/(M_H\omega_M^2)$. For Pt, $\omega_M = 3 \times 10^{13}$ rad/sec and the b_n's [Eq. 120] have been calculated using the aluminum dynamic response function, K.

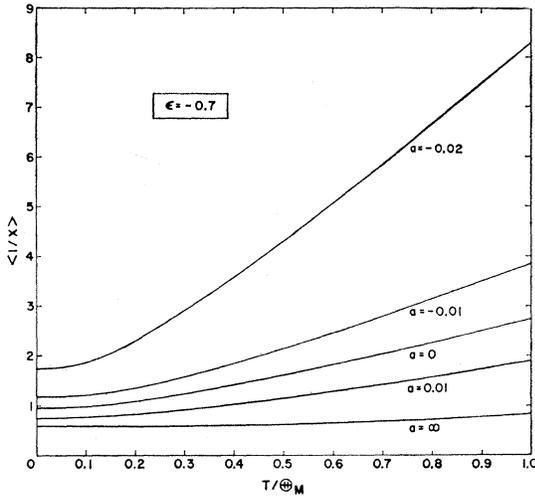| a	x_L	a_L	b_0	b_1	b_2
-0.02	1.012	0.353	0.647	1.411	3.718
-0.01	1.122	0.700	0.300	0.623	1.299
0	1.257	0.839	0.161	0.298	0.761
0.02	1.532	0.927	0.073	0.151	0.486

FIG. 5. Relative mean-square displacement, $\langle 1/x \rangle$, as a function of T/θ_M for Fe^{57} in platinum for various isotropic changes in nearest neighbor force constants. $\theta_M \cong 225°K$.

known, one can use these relations to check the numerical accuracy of a_L and x_L. Our machine calculations were set up to compute all the quantities in Eqs. (119) and (120) and our numerical results are in error by less than 0.1% in all cases computed to date.

The fraction, f, of resonantly absorbed γ rays is given by Eq. (73) instead of $f = e^{-2W}$, due to the localized mode.

V. SUMMARY AND CONCLUSIONS

We have developed techniques in this paper which are suitable for determining the classical motion of an impurity atom harmonically bound in a large crystal when the impurity atom has received a momentum impulse at time $t = 0$. This motion was characterized by a dynamic response function, K. It was also shown that one can express the $g(\mu)$ function, which is needed to determine the total γ-ray cross section of the impurity nucleus, as a simple average over the K function.

We derived expressions for K in terms of the symmetry adapted Green's functions associated with the pure crystal for the cases of an isotopically substituted atom in the germanium lattice and a substitutional impurity atom in the aluminum lattice. We also noted that one should use a Green's function representation in which the molecular vibration symmetry coordinates which coupled with the impurity atom motion serve as basis vectors.

The temperature dependence of the Lamb-Mössbauer coefficient, $2W$, for Sn^{119} substituted isotopically in Ge was calculated and presented in Fig. 2, along with

similar calculations and experimental data on $Sn-Sn^{119}$. The K function for $Ge-Sn^{119}$ was given in Fig. 1 showing that the frequency distribution is pushed to lower frequencies. Consequently, we strongly suspect that the low-temperature heat capacity of $Ge-Sn^{119}$ for low concentrations of Sn^{119} will exhibit marked deviations from that shown by pure Ge. The possibility of detecting the redistribution in frequency by a heat-capacity measurement looks much more promising than the Mössbauer experiment at present.

Our studies to date on an atom substituted into the aluminum lattice have been restricted to Mössbauer measurements with Fe^{57}, although we can easily examine $Al-Au^{197}$ and $Al-Sn^{119}$. Our detailed calculations on $Al-Fe^{57}$ show that an isotopically substituted Fe^{57} nucleus in aluminum should act like a detectable Mössbauer emitter at room temperature. On the other hand, if the Fe^{57} atom is loosely bound it appears as if the resonant fraction of Mössbauer γ rays could be below the level of detection at room temperature but would be observable at liquid-helium temperatures.

We have used the aluminum lattice symmetry adapted Green's function to study the temperature dependence of $2W$ for $Cu-Fe^{57}$ and $Pt-Fe^{57}$ and find that a triply degenerate localized mode occurs for the latter system. On the basis of existing data it appears qualitatively, as if a $Pt-Fe^{57}$ pair is more tightly bound than a $Pt-Pt$ pair.[26]

We also stress the fact that the low-temperature specific heat of aluminum doped with heavy-mass atoms such as Au, Th, or U should show a marked increase over pure aluminum in view of the large shift to lower frequencies in the frequency distribution of those modes strongly coupled to the impurity atom. We are currently calculating the temperature dependence of this heat capacity associated with arbitrary changes in the nearest neighbor force-constant perturbation matrix, κ, for several impurity masses. It is hoped that κ can be bracketed by a combination of Mössbauer studies and heat-capacity studies.

[26] A. H. Muir (private communication).